A Born–Oppenheimer approximation for path integrals with an application to electron solvation in polarizable fluids

J. Cao[a] and B. J. Berne
Department of Chemistry, Columbia University, New York, New York 10027

(Received 8 February 1993; accepted 13 April 1993)

The Born–Oppenheimer approximation is introduced into the path integral expression for the canonical partition function. It is difficult to apply this to simulations. We devise a new adiabatic expression which we call the free energy Born–Oppenheimer approximation which is much easier to simulate. It is shown that this approximation deviates from the exact path-integral expression by no more than does the standard Born–Oppenheimer approximation and we apply it to the problem of an excess electron dissolved in a polarizable fluid.

I. INTRODUCTION

Path integral techniques are very useful for exploring electron and proton solvation and electron transfer in polarizable molecular fluids.[1] The solvated electron or proton is found to sustain energy excitations which are small compared to the energy spacing in the molecular electronic energy levels. This means that the dipolar fluctuations in the molecules, the source of molecular polarizability, are rapid compared to the motions of the solvated electron with a concomitant separation in time scales. These systems can thus be treated in the Born–Oppenheimer (BO) approximation. In this paper we introduce what to our knowledge is a new path integral method for treating the above problems which we call the free energy Born–Oppenheimer (FEBO) approximation.

In a dynamical system with slow and fast degrees of freedom the Born–Oppenheimer approximation consists of solving for the energy eigenvalues and corresponding energy eigenfunctions keeping the slow degrees of freedom fixed. This yields energy eigenvalues and eigenfunctions which are parametrically dependent on the slow degrees of freedom and are called adiabatic states and energy surfaces. The slow degrees of freedom move on these adiabatic energy surfaces and one solves the Schrödinger equation for this motion. In the path integral formalism one then has to perform a separate path integral calculation for each of these adiabatic surfaces. This approach does not readily lend itself to Monte Carlo simulations or to analytical theories using path integrals. In this paper we derive an alternative formulation which does not require separate calculations for each potential energy surface. This formulation is shown to be as accurate as the full Born–Oppenheimer approximation. We apply it to the problem of electron solvation in polarizable fluids but we expect it to be quite useful in other applications.

A useful model for describing polarizable systems is the Drude oscillator model.[2–10] The solvation of an excess electron in a fluid of Drude oscillators is due in large part to the many-body polarization energy. The usual approach is to calculate a pseudopotential describing the electron–atom interaction.[11,12] The pseudopotential consists of a short-range part due to overlap and exchange and a long-range part due to interaction between the electron and the atom. This later term is often taken as a charge-induced dipole interaction $-\alpha e^2 S_w(r)/r^4$ where α is the atomic polarizability and $S_w(r)$ is a switching function. The switching function turns off this polarization interaction at short distance to avoid a divergence. In a fluid it is then necessary to calculate the electrostatic part self-consistently because the field at any given atom is the superposition of the fields due to all the induced dipoles plus the bare field of the electron. We have already treated this problem by full Monte Carlo simulations in the dipole approximation, and by a self-consistent theory due to Lekner,[13] but these treatments are not general. Here we address the problem from a fresh point of view using the FEBO approximation.

In this paper we give a heuristic argument for the new FEBO method and then show that it is as accurate as the original method. We then derive a screening function theory for electron solvation in a fluid of Drude oscillators. Using the FEBO approximation and a normal modes path integral Monte Carlo technique we compare the predictions of this screening function theory to full simulations of electron solvation.

II. THE FREE ENERGY BORN–OPPENHEIMER APPROXIMATION: DERIVATION OF FEBO FROM THE BORN–OPPENHEIMER APPROXIMATION

The Hamiltonian of a system in which x and y are, respectively, the coordinates of the fast and slow degrees of freedom can be written as

$$H = H_x + H_y + V(x,y), \tag{2.1}$$

where H_x and H_y are the corresponding Hamiltonian operators of the uncoupled subsystems and $V(x,y)$ is the coupling potential. In the BO approximation, we follow the standard procedure:[14]

(a) First diagonalize the Hamiltonian $H_x + V(x,y)$ for fixed values of y

$$[H_x + V(x,y)]\psi_l(x|y) = E_l(y)\psi_l(x|y). \tag{2.2}$$

---

[a] In partial fulfillment of the Ph.D. in the Department of Physics, Columbia University.

0021-9606/93/99(4)/2902/15/$6.00

(b) Now solve for the slow variable

$$[H_y+E_l(y)]\chi_{lm}(y)=E_{lm}\chi(y), \tag{2.3}$$

where the eigenvalues $E_l(y)$ from Eq. (2.2) serve as the potential for the slow motion.

The canonical partition function for the whole system in the BO can thus be expressed as a path integral[15]

$$\begin{aligned} Z_{\mathrm{BO}}&=\sum_{lm}\exp(-\beta E_{lm})\\ &=\sum_l\int dy\int_y^y Dy(u)\\ &\quad\times\exp\left(-\beta\int_0^1 du\{H_y+E_l[y(u)]\}\right), \end{aligned} \tag{2.4}$$

where u measures the Euclidean time $t=i\hbar\beta u$. This differs from the usual expression because there is a sum over the states l, moreover, it is not particularly convenient to apply because it requires diagonalization of the fast Hamiltonian. Of course if none of the excited states of the fast motion are thermally excited, Eq. (2.4) will reduce to a simple expression involving only the motion of y on the ground state potential energy surface $E_0(y)$.

Intuitively, factorizing the exponential operators and summing over the states "l" in Eq. (2.4) will lead to a much simpler expression. However, this reduction must be exercised with caution because H_y and $E_l(y)$ do not commute. For any two linear operators A and B, we introduce the well-known identities[16,17]

$$e^{-\beta(A+B)}=e^{-\beta A/2}e^{-\beta C}e^{-\beta A/2} \tag{2.5}$$

and

$$e^{-\beta A/2}e^{-\beta B}e^{-\beta A/2}=e^{-\beta(A+C')}, \tag{2.6}$$

where operators C and C' are defined by $C=B+\hat{L}B$ and $C'=B+\hat{L}'B=(1+\hat{L})^{-1}B$, respectively, where $\hat{L}$ and $\hat{L}'$ are defined to make Eqs. (2.5) and (2.6) exact identities.

Consider the Hamiltonian in Eq. (2.3) and identify H_y as A in Eq. (2.5) and E_l as B in Eq. (2.6), so that

$$\begin{aligned} Z_{\mathrm{BO}}&=\sum_l \mathrm{Tr}\exp[-\beta(H_y+E_l)]\\ &=\mathrm{Tr}\,e^{-\beta H_y/2}\left(\sum_l e^{-\beta C_l}\right)e^{-\beta H_y/2}, \end{aligned} \tag{2.7}$$

where $C_l=E_l+\hat{L}E_l$. Summation over the levels l gives

$$\sum_l e^{-\beta C_l}=\exp[-\beta(F_x+G)], \tag{2.8}$$

where F_x is the free energy of the fast variable at fixed y given by

$$Z_x(y)=\exp[-\beta F_x(y)]=\sum_l\exp[-\beta E_l(y)] \tag{2.9}$$

and G is the correction due to the difference between E_l and C_l. Equation (2.6) can be used to recombine the product to give

$$Z_{\mathrm{BO}}=\mathrm{Tr}\exp[-\beta(H_y+F_x+G+G')], \tag{2.10}$$

in which $G'=\hat{L}'F_x+G$. Obviously, by neglecting the last two terms in the exponent of the right-hand side of the above equation, we can reduce the Born–Oppenheimer approximation to the more convenient path integral form

$$\begin{aligned} Z_{\mathrm{FEBO}}=\int dy\int_y^y[Dy(u)]\exp\Big(-\beta\int_0^1 du\{H_y[y(u)]\\ +F_x[y(u)]\}\Big), \end{aligned} \tag{2.11}$$

an expression that does not involve an explicit sum over l. The path integral for $Z_x(y)$ in Eq. (2.9)

$$\begin{aligned} Z_x(y)=\int dx\int_x^x[\mathscr{D}x(u)]\exp\Big(-\beta\int_0^1\{H_x[x(u)]\\ +V[x(u),y]\}du\Big) \end{aligned} \tag{2.12}$$

is first evaluated in order to obtain the free energy of the fast variable $F_x(y)$ for Eq. (2.11). We call Eq. (2.11) the free energy Born–Oppenheimer (FEBO) approximation or the free energy adiabatic approximation as it requires the evaluation of the free energy of the fast variable (2.9) instead of the summation over l in the standard Born–Oppenheimer approximation (2.4). It should be noted that the action in Eq. (2.11) is purely local in the imaginary time variable u. In the discretized expression, beads at different time slices will not interact through $F_x[y(u)]$.

The difference of the two related but distinct approximations (2.4) and (2.11) depends on $G+G'$. As the above demonstration is quite formal, we now estimate $G+G'$. Recognizing that to lowest order in β,[18]

$$\hat{L}B=\frac{\beta^2}{24}[(B,A),A+2B]+O(\beta^4) \tag{2.13}$$

and $\hat{L}'=-\hat{L}$ to the same order, one obtains the explicit expressions for G and G' to $O(\beta^4)$,

$$G=\frac{\Sigma_l\hat{L}E_l\exp(-\beta E_l)}{\Sigma_l\exp(-\beta E_l)} \tag{2.14}$$

and

$$G'=-\hat{L}F_x. \tag{2.15}$$

Expansion of the commutator [Eq. (2.13)] to the leading order of $O(1/m_y)$ gives

$$\hat{L}E_l=\frac{\beta^2\hbar^2}{12m_y}(\nabla_y E_l)^2, \tag{2.16}$$

where ∂_y is the spatial derivative with respect to the slow variable. Substitution of the above expression into Eqs. (2.14) and (2.15) leads to

$$G+G'=\frac{\beta^2\hbar^2}{12m_y}[\langle(\nabla_y E_l)^2\rangle-\langle\nabla_y E_l\rangle^2], \tag{2.17}$$

where the angular bracket $\langle f\rangle$ denotes the average defined by

$$\langle f\rangle=\frac{\Sigma_l f_l\exp-(\beta E_l)}{\Sigma_l\exp-(\beta E_l)}. \tag{2.18}$$

This is the thermal average of the fast variable, while the slow variable is held fixed.

From the final expression (2.17), it can be concluded that the difference between the two approximations will be very small if one of the following conditions is satisfied:

(a) The mass of the slow variable m_y is large compared to the mass m_x of the fast variable. Path integral simulations based on this have been applied widely to mixed quantum and classical systems.

(b) The ground state of the fast variable dominates. This is the low-temperature limit. For the simulations of electron solvation in polarizable solvents, the Drude oscillators representing the intramolecular electronic degrees of freedom are ground state dominant so that the solvation energy is simply the polarization energy.

(c) The interaction potential is smooth, so that the fluctuation of the force is small.

In contrast to the foregoing, the exact partition function corresponding to Eq. (2.1) involves the summation of x,y paths simultaneously, and after summing over the paths of the fast subsystem, can be cast in the form

$$Z=\int dy \int_y^y [\mathscr{D}y(u)] Z_x[y(u)] \times\exp\left\{-\beta\int_0^1 H_y[y(u)]du\right\}, \qquad (2.19)$$

where $Z_x[y(u)]$ is the influence functional defined by[8]

$$Z_x[y(u)]=\int dx \int_x^x [\mathscr{D}x(u)]\exp\left(-\beta\int_0^1 \{H_x[x(u)] + V[x(u),y(u)]\}du\right). \qquad (2.20)$$

As is well known, the influence functional will give rise to interaction between different time slices of the slow variable y and thus the dynamics of y will be nonlocal in time. Comparison of Eq. (2.12) with Eq. (2.20) indicates that the FEBO approximation [cf. Eq. (2.11)] is equivalent to replacing the influence functional by the simple expression

$$Z_x[y(u)]=\exp\left\{-\beta\int_0^1 F_x[y(u)]du\right\}, \qquad (2.21)$$

so that $F_x(y)$ acts as an effective potential for the slow variable y which becomes local in time. We are able to verify this assumption for quadratic potentials under adiabatic conditions where the separation of time scales of the slow and fast variables is large. Furthermore, we show that the leading nonadiabatic correction is of the form of $\int du \int du' V(u)V(u')$, a term which is shown in Appendix B to give a relative error proportional to the ratio of the time scales.

In Appendix B, a cumulant expansion is used to evaluate the deviation of the FEBO approximation (2.11) from the exact path integral (2.19), and demonstrate that the error is $O(\eta)$, where η is the ratio of the time scales of the slow and fast variables, thus demonstrating that the FEBO is an excellent approximation when there is a wide separation in time scales.

To illustrate the way in which it gives rise to purely local dynamics, we present in Appendix A a simple application of FEBO to a quadratic potential.

III. THE NORMAL-MODE PATH INTEGRAL MONTE CARLO METHOD (NMPIMC)

The free-energy adiabatic approximation we introduced in the last section is applicable to the study of electron solvation in polarizable fluids. However, to apply the adiabatic approximation (2.11), it is necessary to evaluate $Z_x(y)$ of Eq. (2.12) accurately, and this naturally requires an efficient path integral simulation algorithm.

Normal modes have proven useful in the evaluation of path integrals.[15] They have been employed in the study of liquids consisting of quantum Drude oscillators,[6,7,19] in the RISM-polaron theory of electron solvation,[12,20] and in the derivation of the low-temperature variational approximation for the imaginary time quantum propagator.[21,22] The Fourier path integral (FOURPI) method is based on a normal-mode transformation of the kinetic energy contribution to the action.[23,24] It is a simple matter to develop a normal mode path integral Monte Carlo method (NMPIMC) for the simulation of systems with quadratic actions.[25] This is summarized in this section, and it is applied to calculate the ground energy shift of a model potential for the interaction between an electron and polarizable solvent molecules.

A. The discretized normal-mode transformation

The canonical partition function for a one-dimensional quantum particle is[1]

$$Z(\beta)=\lim_{P\to\infty} Z(\beta,P) =\lim_{P\to\infty}\left(\frac{P}{2\pi\lambda^2}\right)^{P/2}\prod_{n=j}^{P}\int dx_j e^{-S(x_j)}, \qquad (3.1)$$

where P is the number of discretization, λ is the thermal wavelength defined as

$$\lambda^2=\frac{\hbar^2\beta}{m}, \qquad (3.2)$$

and $S(x_i)$ is the imaginary time (or Euclidean) action given by

$$S(x_j)=\sum_{j=1}^{P}\frac{P}{2\lambda^2}(x_j-x_{j-1})^2+\frac{\beta}{P}\sum_{j=1}^{P}V(x_j), \qquad (3.3)$$

where $x_P=x_0$. The underlying idea of the staging method,[26] the Fourier coefficient method,[24] and also the normal-mode method is to generate the configurations from the quantum kinetic energy part of the Euclidean action, i.e., the first term in Eq. (3.3), so that the stiff polymer chain can be sampled much more efficiently with the improved methods than with the primitive method. The configuration thus generated is accepted or rejected according to the Metroplis importance sampling of the potential energy part of the Euclidean action, i.e., the second term in Eq. (3.3).

The normal-mode transformation is defined as

$$x_j=\sum_{n=1}^{P} a_n \exp\left(-\frac{i2\pi jn}{P}\right), \tag{3.4}$$

where a_n is the normal-mode coordinate. Using the orthonormal relation $\Sigma_{m=1}^{P}\exp\{[i2\pi m(l-n)]/P\}=P\delta_{nl}$, we are able to diagonalize the kinetic part of the imaginary time action

$$\sum_{j=1}^{P} \frac{P}{2\lambda^2}(x_j-x_{j-1})^2=\sum_{n=1}^{P} \frac{2P^2[1-\cos(2\pi n/P)]}{\lambda^2}|a_n|^2, \tag{3.5}$$

where the set of Gaussians $|a_n|^2$ can be easily generated by the box Muller technique. To shorten the computer time to perform the transformation (3.3), we take $P=2^n$ and make use of the fast Fourier transformation technique. If the action is purely quadratic,

$$S(x_j)=\sum_{j=1}^{P} \frac{P}{2\lambda^2}(x_j-x_{j-1})^2+\frac{\beta m\omega^2}{2P}x_j^2, \tag{3.6}$$

where ω is the intrinsic frequency of the linear harmonic oscillator. The transformation (3.4) leads to

$$S(a_n)=\sum_{n=1}^{P}\frac{|a_n|^2}{2\lambda_n^2}, \tag{3.7}$$

where λ_n^2 is expressed as

$$\lambda_n^2=\frac{\lambda^2}{2P^2[1-\cos(2\pi n/P)]+b^2}, \tag{3.8}$$

in which the parameter $b=\hbar\beta\omega$ measures the effect of quantum mechanics. Notice Eqs. (3.7) and (3.8) take the same form as Eq. (3.5) except for the introduction of parameter b. This implies that the Monte Carlo sampling method is the same as for the free particle propagator (3.5) after we redefined the Gaussian width according to Eq. (3.8).

The fact that $\{x_j\}$ are real requires that the complex variables $\{a_n = a_n' + ia_n''\}$ satisfy the following constraints: $a_n^* = a_{P-n}$ and $a_P^* = a_P$, so that there are P independent degrees of freedom. Thus, we can rewrite Eq. (3.5) as

$$\begin{aligned} S(a_n)&=\sum_{n=1}^{P}\frac{|a_n|^2}{2\lambda_n^2}\\ &=\sum_{n=1}^{P/2-1}\left[\frac{(a_n')^2+(a_n'')^2}{\lambda_n^2}\right]+\left[\frac{(a_{P/2}')^2}{2\lambda_{p/2}^2}+\frac{(a_P')^2}{2\lambda_P^2}\right], \end{aligned} \tag{3.9}$$

where λ_n is the thermal wavelength of the nth normal mode given by Eq. (3.8). It is obvious from Eq. (3.9) that the Gaussian widths for the real part a_n' and imaginary part a_n'' for the first $P/2-1$ modes are λ_n, whereas $a_{P/2}$ is real with Gaussian width $\sqrt{2}\lambda_{P/2}$, and a_P is real with Gaussian width $\sqrt{2}\lambda_P$. The variables from $P/2+1$ to $P-1$ can be obtained by taking the complex conjugate of the first $P/2-1$ variables according to $a_n^* = a_{P-n}$.

Further development can be achieved by taking advantage of the fact that the exact propagator of the quantum linear harmonic oscillator is known. A harmonic reference system can thus be employed in umbrella sampling. The idea is to separate the full potential V into a reference potential V_0 and a residue potential $V'=V-V_0$. After substituting the exact propagator for the reference LHO potential, the quantum partition function for the full Hamiltonian is

$$\begin{aligned} \lim_{P\to\infty} Z(\beta,P)=\lim_{P\to\infty}\left(\frac{P}{2\pi\lambda'^2}\right)^{P/2}\prod_{n=j}^{P}\int dx_j\, e^{-S_0(x_j)}\\ \times\exp\left[-\frac{\beta}{P}\sum_j V'(x_j)\right], \end{aligned} \tag{3.10}$$

where the thermal wavelength λ' is defined by $\lambda'^2=[(\hbar^2\beta)/m]\{[\sinh(R)]/R\}$ in which $R=b/P$, and the imaginary time action for the reference LHO is

$$S_0(x_j)=\sum_{j=1}^{P}\frac{P}{2\lambda'^2}[(x_j^2+x_{j-1}^2)\cosh(R)-2x_jx_{j-1}]. \tag{3.11}$$

Notice that in the limit where $R\to b/P$ becomes infinitesimally small, the action reduces to Eq. (3.6).

If we introduce a new set of parameters λ' and $b'=b\{[\sinh(R/2)]/[(R/2)]\}$, the imaginary time action S_0 of Eq. (3.11) reduces to $S_0(a_n) = \Sigma_{n=1}^{P}(|a_n|^2/2\lambda_n'^2)$ as in Eq. (3.7) with λ_n' defined by

$$\lambda_n'^2=\frac{\lambda'^2}{2P^2[1-\cos(2\pi n/P)]+b'^2}. \tag{3.12}$$

The normal-mode configurations are generated by P Gaussians defined by their Gaussian widths [Eq. (3.12)], and transformed back to the real coordinates through Eq. (3.4). Then, the residue potential V' is evaluated and used as the criterion of the Metroplis importance sampling. In Appendix D, we will give the virial estimator for Eq. (3.10).

B. The evaluation of convergence

Since the action in Eq. (3.11) is exact for the LHO potential, convergence of the partition function when $V'=0$ will be independent of P. In order to estimate and compare the rate of convergence for the free particle propagator (3.3) with the exact LHO propagator (3.11), we take the example of a solvable model $V'=gx^2$. By defining the frequency for the full potential as

$$\bar{\omega}=\omega\sqrt{1+\frac{2g}{m\omega^2}}, \tag{3.13}$$

we readily obtain the energy expectation value for the primitive propagator Eq. (3.1)

$$E(\beta,P)=\frac{\hbar\omega}{2}\frac{1}{\sqrt{1+R^2/4}}\frac{f^P+1}{f^P-1}, \tag{3.14}$$

where $R=b/P$ and $f = 1 + r^2/2 + R\sqrt{1+R^2/2}$.

A close examination of the imaginary time action with the exact LHO action

$$S(x_j)=\sum_{j=1}^{P}\frac{PR}{2\lambda^2\sinh(R)}(x_j-x_{j-1})^2+\sum_{j=1}^{P}\left[\frac{PR}{\lambda^2}\frac{\cosh(R)-1}{\sinh(R)}+\frac{g\beta}{P}\right]x_j^2, \tag{3.15}$$

leads us to define

$$\bar{R}^2=[2\sinh(R/2)]^2+\frac{2g\lambda^2\beta\sinh(R)}{P^2R} \tag{3.16}$$

and $\bar{\lambda}=\lambda'$. With these changes of parameters, the energy expectation value is expressed as

$$E(\beta,P)=\frac{1}{\sqrt{1+\bar{R}^2/2}}\frac{\bar{f}^P+1}{\bar{f}^P-1}\left(\frac{P}{2}\frac{\partial\bar{R}}{\partial\beta}\right). \tag{3.17}$$

As an example, we take $b=10.0$ and $g/(m\omega^2)=0.1$ and calculate the energies which we plot as a function of the number of beads (P) in Fig. 1. The dotted curve is the exact energy; the solid curve is the energy of the primitive propagator evaluated from Eqs. (3.13) and (3.14), and the bold curve is the energy of the LHO reference propagator evaluated from Eq. (3.17). This example clearly shows that the LHO reference propagator is superior to the primitive propagator.

IV. SOLVATION ENERGY OF AN ELECTRON IN A POLARIZABLE FLUID

Polarizable fluids pose a difficult problem in many-body physics. It is becoming increasingly clear that electrical induction has an important effect in fluids such as water, where the induced dipoles can be 50% as large as the permanent dipoles.[27,28] The electronic charge distribution in a real molecule or atom is continually fluctuating. This electronic motion is often modeled by a harmonic oscillator with a frequency ω_0, mass μ, charge q, and instantaneous dipole $\mathbf{p}$. If the electrostatic interaction is approximated by the dipolar interaction, the problem reduces to a matrix problem.[29] Usually ω_0 is assumed to be high compared to the characteristic time scale of the nuclear motion, so that the varying dipole can quickly respond to the changing environment, and a Born–Oppenheimer approximation is valid.

When an excess electron is inserted in the polarizable system, the charge–dipole interactions lead to electron solvation. Both the Drude dispersion oscillators and the excess electron must be treated quantum mechanically, whereas the motions of the heavy nuclei can usually be treated classically. The task of calculating the polarization energy is definitely beyond the current capability of simulations. The problem is simplified enormously by the following procedure:

(a) The fact that the excitation energy of the solvated electron is small compared to the excitation energy of the Drude oscillator[1,20,30] suggests that FEBO can be applied with the solvated electron treated as the slow system and the Drude oscillators treated as the fast system. F_x of Eq. (2.21) is then the solvation free energy of a classical electron in the polarizable fluid.

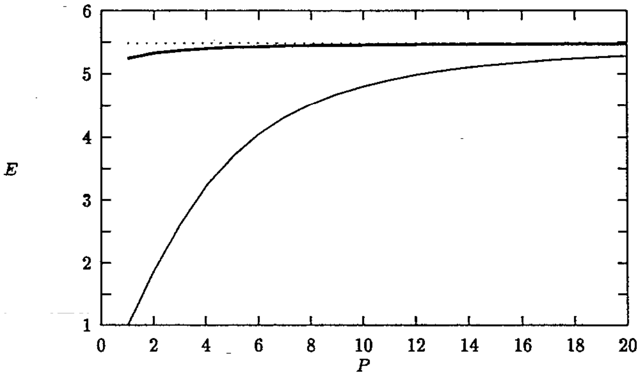

FIG. 1. The dependence of the mean energy on the number beads P. (a) The dotted curve is the exact energy from Eq. (3.13); (b) the solid curve is the energy of the primitive propagator evaluated from Eqs. (3.13) and (3.14); (c) the bold curve is the energy of the LHO reference propagator evaluated from Eq. (3.17).

(b) The calculation of the full Coulombic free energy of a classical electron interacting with a fluid of polarizable molecules is difficult. For simplicity, we first calculate the Coulomb interaction energy of a classical electron with a single quantum Drude oscillator using NMPIMC method outlined in Sec. IV A.

(c) The solvation energy of a classical electron dissolved in a fluid of polarizable spheres is calculated by introducing a screening function[11,13] which incorporates many-body interactions based on the full Coulomb interaction between the electron and a single Drude oscillator contribution determined in step (b).

A. Application of the FEBO to polarizable systems

An excess electron interacting with a polarizable fluid can be exactly treated in the dipole approximation by matrix techniques.[29] The Hamiltonian for the system consists of kinetic energy terms, intramolecular polarization energy terms corresponding to the energy required to distort the drude oscillators, dipole–dipole interaction energy terms for the interactions between the spontaneous dipoles on all of the Drude oscillators, and finally the interactions between the Drude oscillators and the excess electron. These interactions give rise to the following partition function which we shall show can be reduced to the form of Eq. (2.21).

The imaginary time path integral representation of the quantum partition function of the Drude oscillator system in the electric field of the electron is

$$Z_{qm}[(\mathbf{R}_i)]=\int\mathscr{D}\mathbf{p}(u)\exp\left(-\beta\int_0^1 du\left\{\sum_i\frac{1}{2\alpha b^2}\left[\frac{\partial\mathbf{p}_i(u)}{\partial u}\right]^2+\sum_i\frac{\mathbf{p}_i^2(u)}{2\alpha^2}-\sum_{i>j}\mathbf{p}_i(u)\cdot\mathscr{T}_{ij}\cdot\mathbf{p}_j(u)-\sum_i\mathbf{E}_i(u)\cdot\mathbf{p}_i(u)\right\}\right), \tag{4.1}$$

where indices i and j stand for particles and $\mathscr{T}$ is the dipolar matrix defined as

$$\mathscr{T}_{ij}^{\mu\nu}=\frac{3R_{ij}^{\mu}R_{ij}^{\nu}-\delta^{\mu\nu}R_{ij}^{2}}{R_{ij}^{5}}, \tag{4.2}$$

in which R_{ij} is the vector connecting particle i and particle j. Equation (4.1) is the Drude oscillator part of quantum partition function we introduced in the previous paper. Transformation to the normal-mode coordinates

$$p_i(u)=\sum_{n=-\infty}^{n=\infty}\tilde{p}_{i,n}e^{-i2\pi nu} \tag{4.3}$$

diagonalizes the kinetic and quadratic potential terms allowing immediate integration of each mode independently. The quantum partition function takes the form of a product of classical partition functions for the individual modes[19]

$$Z_{qm}[(R_i)]=\sum_{n=-\infty}^{\infty}Z_{\mathrm{cl}}^{n}[(R_i)], \tag{4.4}$$

where the partition function for a particular mode is

$$Z_{\mathrm{cl}}^{n}[(R_i)]=\left[\left(\frac{2\pi\alpha_n}{\beta}\right)^{N}\frac{1}{\det\mathscr{A}_n}\right]^{1/2}\times\exp\left[\frac{1}{2}\beta\sum\alpha_n\mathbf{E}_{i,n}^{*}\cdot(\mathscr{A}_n)_{ij}^{-1}\cdot\mathbf{E}_{j,n}\right] \tag{4.5}$$

in which $\mathbf{E}_{i,n}$ is the normal-mode transformation of the electrostatic field at particle i, α_n is the generalization of the classical static polarizability

$$\frac{1}{\alpha_n}=\frac{1}{\alpha}\left[\left(\frac{2\pi n}{b}\right)^{2}+1\right], \tag{4.6}$$

and $\mathscr{A}_n$ is defined as

$$\mathscr{A}_n=\mathscr{I}-\alpha_n\mathscr{T}. \tag{4.7}$$

Obviously, for $n=0$, α_n reduces to the classical polarizability α.

The prefactor in Eq. (4.5) $[(2\pi\alpha_n/\beta)^N/(\det\mathscr{A}_n)^{1/2}]$ gives the quantum many-body dispersion energy of the system which adds to the two-body repulsive energy given by the first term. In simulations, only the two-body part of the dispersion interaction is usually included by incorporating it into the simple pairwise potentials, but it should be recognized that the above expression contains many-body effects to all orders. In another paper,[29] we reported simulation results on clusters and liquids when many-body dispersion forces are treated using the matrix formulation and the normal-mode transformation developed here.

The exponential term gives the quantum polarization energy due to the interaction of the Drude oscillators with the bare Coulombic fields arising either from permanent monopoles or external fields. This quantum polarization energy is

$$\Phi_P[(R_i)]=-\frac{1}{2}\sum_{n=-\infty}^{+\infty}\alpha_n\sum_{ij}E_{i,n}\cdot(A_n^{-1})_{ij}\cdot E_{j,n}, \tag{4.8}$$

where the electric field arising from a quantum particle like an electron is quantized and is given by $\mathbf{E}_{i,n}$, the normal-mode transformation of the electronic field. Every term of the Taylor expansion of $\mathscr{A}_n$ can be transformed back to the imaginary time space individually with α_n^{m+1} being converted to a correlation function. Then writing

$$\hat{\alpha}_m(u)=\sum_n e^{-2\pi nu}\alpha_n^{m+1}, \tag{4.9}$$

the polarization energy (4.8) can be expressed as

$$\sum_{m=0}^{\infty}\sum_n\frac{\beta}{2}\alpha_n^{m+1}\mathbf{E}_{i,n}^{*}\cdot\mathscr{T}_{i,j}^{m}\cdot\mathbf{E}_{j,n}=\frac{\beta}{2}\sum_{m=0}^{\infty}\int_0^1 du\int_0^1 du'\alpha_m(u-u')\mathbf{E}_i(u)\mathscr{T}_{i,j}^{m}\cdot\mathbf{E}_j(u'). \tag{4.10}$$

Let us investigate the first term in the expansion, the $m=0$ term. As

$$\hat{\alpha}_0(u)=\alpha b\frac{\cosh[(b/2)-bu]}{2\sinh(b/2)}, \tag{4.11}$$

in the extreme quantum limit $b\rightarrow\infty$, $\hat{\alpha}$ reduces to

$$\lim_{b\rightarrow\infty}\hat{\alpha}_0(u)=\tfrac{1}{2}[\delta(u)+\delta(1-u)], \tag{4.12}$$

where the variable u, defined over the domain (0,1), is periodic. Thus the leading term ($m=0$) in Eq. (4.10) is

$$\frac{1}{2}\int_0^1\int_0^1\alpha(u-u')\mathbf{E}(u)\mathbf{E}(u')du\,du'=\frac{\alpha}{2}\int_0^1\mathbf{E}^2(u)du, \tag{4.13}$$

where the periodic property of the electrical field $\mathbf{E}(u)$ on (0,1) is implied.

The next term ($m=1$) involves two-body interactions. The summation can be carried out by contour integration giving

$$\hat{\alpha}_1(u)=\alpha^2\left\{\frac{b}{4}\frac{\cosh[(b/2)-bu]}{\sinh(b/2)}\left[1+\frac{b}{2\tanh(b/2)}\right]-\frac{b^2}{8}(1-2u)\frac{\sinh[(b/2)-bu]}{\sinh(b/2)}\right\}. \tag{4.14}$$

Again, the above expression reduces to a delta function in the $b\rightarrow\infty$ limit.

In general, all ($\hat{\alpha}_m$) reduce to delta functions in this limit because the electronic field correlation function changes very little in the interval $\hbar\omega\beta$. This follows whenever the level spacings ($\hbar\omega$) of the harmonic oscillators are much larger than the level spacings of the solvated electron. In this limit, there is an adiabatic separation in the time scales of the fast polarization fluctuations and the slow electron fluctuations. Then the polarization energy becomes

$$\Phi_P[(\mathbf{R}_i)]=-\frac{\alpha}{2}\int_0^1 du\,\mathbf{E}_i(u)\cdot\mathscr{A}_{i,j}^{-1}\cdot\mathbf{E}_j(u), \tag{4.15}$$

which can be viewed as the generalization of the FEBO [Eq. (2.11)] to many-body dipolar systems.

Although Eq. (4.15) was derived in the dipolar approximation, the conclusion is more general and is essentially the FEBO approximation applied to the many-body solvation problem. Equation (4.15) gives the polarization energy for a given electron path. Thus when the electron path is discretized, the quantum solvation energy is the average of the solvation energy of each individual electron bead

$$\Phi_P^{qm}[(\mathbf{R}_i)] = \int_0^1 \Phi_P^{\mathrm{cl}}[(\mathbf{R}_i),u]du. \tag{4.16}$$

This is exactly the algorithm used by Berne *et al.*[11] in their computer simulation of the many-body polarization effect of an electron solvated in water and liquid Xe. The above approximation can be generalized to simulate any complicated system with two different time scales.

B. The ground state energy of an electron and a Drude oscillator

We now study the simple problem of a highly quantum mechanical Drude oscillator of mass m, frequency ω, and charge q with [$\omega=0.534$, $m=0.245$, and $q=1.38$) (which are the parameters of Xe (Ref. 31)] in the Coulomb field of an electron fixed in the space. We calculate the quantum ground state energy shift of the oscillator ΔE due to the electron. The positive charge of the Drude oscillator is placed at the origin (0,0,0), while the negative charge is oscillating under the linear harmonic potential. The electron is placed at distance R on the x axis $(R,0,0)$. The potential is then

$$V(\mathbf{r}) = \frac{1}{2} m\omega^2 \mathbf{r}^2 - eq\left(\frac{1}{R} - \frac{1}{|\mathbf{R}-\mathbf{r}|}\right), \tag{4.17}$$

where $\mathbf{r}$ is the displacement of the negative charge of the Drude oscillator. At room temperature ($T=309$ K), $b=\beta\hbar\omega=545$, this oscillator is ground state dominated so that the ground state energy shift is the same as the solvation energy Φ_P^{cl} of Eq. (4.16) or equivalently F_x of Eq. (2.11).

The slow variable (the solvated electron) always moves on the ground state energy surface determined by the fast variable (the Drude oscillator), and hence the free energy adiabatic approximation and the ordinary adiabatic approximation are equivalent and can both give the exact result. For large $\beta\hbar\omega$, the free energy (2.9) and the ground state energy (2.3) will be the same. Thus the diffusion Monte Carlo (DMC) method can be used to obtain the ground state energy shift δE for comparison with the FEPIMC method (a quantum perturbation calculation is presented in Appendix D). Path integral simulations are usually used to study temperature-dependent properties and are generally not efficient for calculating ground state energies, nevertheless, we find that NMPIMC is at least as effective as the DMC for calculating the ground state energy for the potential (4.17).

The calculation of the ground energy shift caused by a small perturbation requires the simulation of a system with a large number of beads and requires very long runs because an accurate determination of the difference between two large expectation values is required. One way to circumvent this difficulty is to use the residue potential $V'=V-V_0$ as a weighting function instead of a Metroplis importance sampling function as in Eq. (3.10), and V_0 is the quadratic reference potential given in Eq. (3.6). This gives

$$Z'(\beta,P) = \left\langle \exp\left[-\frac{\beta}{P}\sum_j V'(x_j)\right]\right\rangle, \tag{4.18}$$

where the average is taken over the configurations generated by e^{S_0} of Eq. (3.11). In the limit of low temperature, Z' yields the ground energy shift due to V'

$$\Delta E = -\lim_{\beta\to\infty}\lim_{P\to\infty} \ln Z'(\beta,P). \tag{4.19}$$

For the potential (4.17), if $b\geqslant 5$ and $P\geqslant 2^6$, the difference between the exact ground state energy and the average energy is beyond the resolution of single precision on the computer.

The potential (4.17) has a singularity at $\mathbf{r}=\mathbf{R}$. In order to avoid the divergence, we have to include a higher order correction term in the action which is a short range repulsive force[18]

$$V'' = V' + \frac{1}{24}\frac{\hbar^2\beta^2}{mP^2}(\nabla V')^2, \tag{4.20}$$

which is to be used in Eq. (4.18) instead of V'. The high order term vanishes at long range $O(1/r^4)$, but it speeds up the convergence.

There are two additional advantages to the use of the NMPI Monte Carlo method:

(a) We observe that the LHO reference potential is isotropic, but the interaction potential in Eq. (4.17) is different in the perpendicular and parallel directions to the $\mathbf{R}$ axis. Therefore for each set of normal modes, there exist six arrangements which are the same configuration for the reference LHO potential, but different configurations for the Coulombic interaction potential. This implies that for each configuration generated by the reference system e^{-S_0}, we can obtain six statistically independent weights $e^{-\beta V'}$ by permutation and reverse transformations. This saves computation time because the configuration generation and the normal-mode transformation is the most time-consuming part of the algorithms.

(b) The distance R in Eq. (4.17) only appears in the interaction potential V', whereas the LHO reference potential is independent of R, so that the same configuration generated from the reference potential can be used to calculate the interaction potential at all the separations. It is thus possible to obtain δE as a function of the separation R by performing a single Monte Carlo simulation.

We perform NMPIMC simulations at $b=5$ and $P=64$. 10^6 independent configurations are sampled. The energy correction function $c(R)$ is defined as

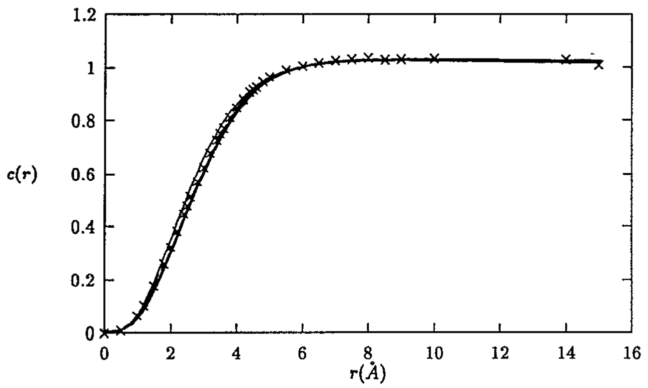

FIG. 2. The correction function $c(r)$ defined by Eq. (4.21). (a) The bold curve is the NMPIMC results [cf. Eq. (4.19)]; (b) the solid curve is the results of the quantum perturbation calculation (D15) (cf. Appendix E); (c) the results of diffusion Monte Carlo calculations are given by "×".

$$c(r)=\frac{\Delta E}{\Delta E_d}, \tag{4.21}$$

where $\Delta E_d=-\alpha e^2/2R^4$ is the energy shift if only the dipole interaction is included.

In Fig. 2, $c(R)$ thus obtained is plotted from $R=0.5$ to $R=15.0$ (the bold curve). For the sake of comparison, we also plot the results of a quantum perturbation calculation [Eq. (E15)] (cf. Appendix E) and the results of a diffusion Monte Carlo calculation[32] for the same potential Eq. (4.17).

C. Screening function theory for electron solvation in polarizable fluids

In this section, we derive the screening function for the solvated electron in polarizable fluids. We start by considering only charge–dipole and dipole–dipole interactions. Then the electron-Drude oscillator interacting is

$$V_{\text{int}}=-\sum_i \mathbf{p}_i\cdot\mathbf{E}_i, \tag{4.22}$$

in which $\mathbf{E}_i=-e\mathbf{r}_i/r_i^3$ is the bare electric field at Drude oscillator i due to the electron at the origin. The polarization energy for a given configuration of Drude oscillators in the adiabatic approximation [cf. Eq. (4.15)] is then

$$\Phi_P=-\frac{1}{2}\sum_{ij}\alpha\mathbf{E}_i\cdot(\mathscr{I}-\alpha\mathscr{T})_{ij}^{-1}\cdot\mathbf{E}_j=-\frac{1}{2}\sum_i \mathbf{E}_i\cdot\mathbf{E}_i^t, \tag{4.23}$$

where $\mathscr{T}_{ij}$ is the dipolar propagator. $\mathbf{E}_i^t$ in Eq. (4.23) is the total field at atom i given by

$$\mathbf{E}_i^t=\mathbf{E}_i+\alpha\mathscr{T}_{ij}\cdot\mathbf{E}_j^t \tag{4.24}$$

or

$$\mathbf{E}_i^t=\sum_j(\mathscr{I}-\alpha\mathscr{T})_{ij}^{-1}\cdot\mathbf{E}_j, \tag{4.25}$$

so that in a simulation, $\{\mathbf{E}_i^t\}$ can be determined by interaction or by matrix inversion (usually used for small samplers and clusters).

The field at point $\mathbf{r}$ is defined as

$$\hat{\rho}(\mathbf{r})\hat{\mathbf{E}}(\mathbf{r})=\sum_i\delta(\mathbf{r}-\mathbf{r}_i)\mathbf{E}_i, \tag{4.26}$$

where $\hat{\rho}(\mathbf{r})=\Sigma_i\delta(\mathbf{r}-\mathbf{r}_i)$ is the instantaneous number density. This allows us to express the field equation as

$$\hat{\rho}(\mathbf{r})\hat{\mathbf{E}}^t(\mathbf{r})=\hat{\rho}(\mathbf{r})\hat{\mathbf{E}}(\mathbf{r})+\alpha\int d\mathbf{r}'\hat{\rho}(\mathbf{r})\hat{\rho}(\mathbf{r}')\mathscr{T}(\mathbf{R})\cdot\hat{\mathbf{E}}^t(\mathbf{r}'), \tag{4.27}$$

where $\mathbf{R}=\mathbf{r}-\mathbf{r}'$ and $\mathscr{T}$ is the dipolar propagator defined by Eq. (4.4).

A mean field approximation can be invoked by taking

$$\langle\hat{\rho}(\mathbf{r})\hat{\mathbf{E}}^t(\mathbf{r})\rangle=\rho(\mathbf{r})\mathbf{E}^t(\mathbf{r}), \tag{4.28}$$

where $\rho(\mathbf{r})$ and $\mathbf{E}^t(\mathbf{r})$ is the configuration averaged density and the field at $\mathbf{r}$ given that the electron is at the origin. Averaging Eq. (4.27) over fluid configurations gives

$$\rho(\mathbf{r})\mathbf{E}^t(\mathbf{r})=\rho(\mathbf{r})\mathbf{E}(\mathbf{r})+\alpha\int d\mathbf{r}'\rho_2(\mathbf{r},\mathbf{r}')\times[\mathscr{T}(\mathbf{R})\cdot\mathbf{E}^t(\mathbf{r}')], \tag{4.29}$$

where we assumed $\langle\hat{\rho}(\mathbf{r}')\hat{\rho}(\mathbf{r})\hat{\mathbf{E}}^t(\mathbf{r}')\rangle=\rho_2(\mathbf{r},\mathbf{r}')\mathbf{E}^t(\mathbf{r}')$, where ρ_2 is the distribution function of one solvent particle at $\mathbf{r}$ and another at $\mathbf{r}'$,

$$\rho_2(\mathbf{r},\mathbf{r}')=\left\langle\sum_{i\neq j}\delta(\mathbf{r}-\mathbf{r}_i)\delta(\mathbf{r}'-\mathbf{r}_j)\right\rangle. \tag{4.30}$$

A further approximation is to invoke the Kirkwood superimposition approximation

$$\rho_2(\mathbf{r},\mathbf{r}')=\rho(\mathbf{r})\rho(\mathbf{r}')g(\mathbf{R}), \tag{4.31}$$

where $g(\mathbf{R})$ is the solvent–solvent pair correlation function assuming the solvent structure is unperturbed by the electron.

In an isotropic fluid, the resulting average total field must be along the same direction as the original field. So we introduce a screening function $f(r)$ as

$$f(r)\equiv\frac{|\langle\mathbf{E}^t\rangle|}{|\mathbf{E}|}, \tag{4.32}$$

which measures the screening effect due to the many-body polarization. Therefore after substitution of Eqs. (4.31) and (4.32), the average field equation (4.29) becomes the equation for the screening function

$$f(r)=1+\alpha\rho\int d\mathbf{r}'[\mathbf{n}_r\cdot\mathscr{T}(\mathbf{R})\cdot\mathbf{n}_{r'}]g(R)f(r')g_e(r')\frac{r^2}{r'^2}, \tag{4.33}$$

in which ρ is the density of the fluid, $g(R)$ is the pair correlation function between solvent particles, and $g_e(r)$ is the pair correlation function between the solvent particle and the electron.

The mean field equation approximates the average after the integration which requires an exact many-body solution. In Eq. (4.33), only two-body correlation functions are involved and this suggests an approximation that all the high-order many-body correlation functions are products of two-body correlation functions. Nevertheless, as we shall see, Eq. (4.33) provides a reasonable approximation to the screening function and can be easily generalized to more complicated situations.

Now we take into account the full Coulomb interaction between the electron and the Drude oscillator given in Eq. (4.17). It is extremely time consuming to calculate solvation energy between the classical electron and the quantum Drude fluid by any simulation method. Moreover, the calculation must be repeated for every nuclear configuration and every electron chain configuration. Fortunately, we can incorporate the correction function calculated for a single Drude oscillator and the mean field approximation for the screening function (4.33) to obtain the solvation energy. There are two approaches.

A relatively easy approach is to introduce an effective field $\mathbf{E}^e$. Presumably the effective field accounts for the energy shift ΔE we calculated in last section, i.e., $\mathbf{E}^e = \sqrt{c(r)}\mathbf{E}$. Then the formula (4.24) is still valid after a little modification—replacing E by E^e. The polarization energy is

$$\Phi_P = -(1/2)\alpha \sum_i E^2(r_i) f(r_i) c(r_i) \tag{4.34}$$

and the screening function $f(r)$ is

$$f(r) = 1 + \alpha\rho \int d\mathbf{r}' [\mathbf{n}_r \cdot \mathscr{T}(\mathbf{R}) \cdot \mathbf{n}_{r'}] \times g(R) f(r') g_e(r') \frac{r^2 \sqrt{c(r')}}{r'^2 \sqrt{c(r)}}. \tag{4.35}$$

This equation can be solved by iteration. If $g_e(r)$ is set equal to unity and $c(r)$ is replaced by a phenomenological switching function $S_w(r)$, this equation reduces to the mean field theory of Lekner,[13] a screening theory that has been used in previous simulations. It has been shown that in fluids such as xenon, where the electron solvates in an extended state and therefore does not perturb the fluid structure, the Lekner theory agrees with a full simulation based on inclusion of full many-body electrical induction in the dipolar approximation to within 10%. Equation (4.35) is more general and allows for the possibility that the fluid structure is perturbed by the excess electron. It also includes the correction factor $c(r)$ which approximately converts the dipole interaction to one that includes the full Coulomb interaction. From this, it can be seen that the introduction of a switching function in the Lekner theory is equivalent to introducing this correction factor $c(r)$.

The second approach is to introduce an effective polarizability. The electric field of the excess electron distorts the Drude oscillators, inducing not only a dipole, but also a quadrapole and other high order multipoles. We approximate these induced multipoles by introducing an effective polarizability tensor. Expanding the Coulomb interaction energy to the second order in the displacement of the Drude oscillator, we have

$$H = \sum_i \frac{\dot{\mathbf{p}}_i^2}{2\alpha\omega^2} + \sum_i \frac{\mathbf{p}_i^2}{2\alpha} - \sum_i \frac{1}{2} \mathbf{p}_i \cdot \mathscr{S}_i \cdot \mathbf{p}_i - \sum_{ij} \frac{\mathbf{p}_i \cdot \mathscr{T}_{ij} \cdot \mathbf{p}_j}{2} - \sum_i \mathbf{p}_i \cdot \mathbf{E}_i, \tag{4.36}$$

where $\mathscr{S}$ introduces the effect of the electron on the fluctuation of the Drude oscillator. The tensor $\mathscr{S}$ is given by $\mathscr{S} = -a\mathscr{D}$, where a is the constant $a = e/qR^3$ and $\mathscr{D}$ is the tensor $\mathscr{D} = 3\mathbf{nn} - \mathscr{I}$.

If we ignore the energy shift due to the frequency shift, the polarization energy can be expressed as

$$\Phi_P = -\alpha \sum_i \mathbf{E}_i \cdot \mathscr{B}_i \cdot \mathbf{E}_i^t, \tag{4.37}$$

and the total field $\mathbf{E}^t$ as

$$\mathbf{E}_i^t = \mathbf{E}_i + \alpha \mathscr{T}_{ij} \cdot \mathscr{B}_j \cdot \mathbf{E}_j^t, \tag{4.38}$$

where $\alpha\mathscr{B}_j$ serves as the effective polarizability tensor defined as

$$\mathscr{B} = (\mathscr{I} - \alpha\mathscr{S})^{-1}. \tag{4.39}$$

We can express the tensor explicitly as

$$\mathscr{B} = \frac{1+b}{(1+2b)(1-b)} \left(\mathscr{I} - \frac{b}{1+b} \mathscr{D} \right), \tag{4.40}$$

in which $b = \alpha a$.

It should be noted that

$$\mathscr{B} \cdot \mathbf{n} = \frac{1}{1+2b} \tag{4.41}$$

is exactly the correction factor $c(r)$ given by Eq. (E6). Therefore we can identify the factor $\mathscr{B}$ with the correction function $c(r)$.

Averaging over fluid configurations, and assuming that the total field is parallel to $\mathbf{n}$, the direction of the bare field $\mathscr{B}\mathbf{E}^t$ can be replaced by $c(r)\mathbf{E}^t$. Then the equation for the screening function $f(r)$ is

$$f(r) = 1 + \alpha\rho \int d\mathbf{r}' [\mathbf{n}_r \cdot \mathscr{T}(\mathbf{R}) \cdot \mathbf{n}_{r'}] \times g(R) f(r') g_e(r') \frac{r^2 c(r')}{r'^2} \tag{4.42}$$

and the polarization energy is calculated using Eq. (4.34).

The Hamiltonian in Eq. (4.36) is very much the same as the illustrative quadratic model [cf. Eq. (A4)] if we identify $\mathscr{S}$ as W in Eq. (A4) and $\mathscr{B}$ as C in Eq. (A8), except here Eq. (4.36) corresponds to a many-body system. The adiabatic expression (A22) includes contributions from the frequency shift which we take into some account by introducing the correction function $c(r)$ for a single Drude oscillator, thus ignoring the many-body quantum interference in the energy shift.

In Fig. 3, screening functions calculated from Eqs. (4.35) and (4.42) are plotted for a hard sphere fluid of reduced density $\rho^* = \rho\sigma^3 = 0.8$ and reduced polarizability $\alpha^* = \alpha/\sigma^3 = 0.06$. $\sigma = 0.767$ Å is the hard-sphere diameter of the solvent atoms (Xe). The pair correlation func-

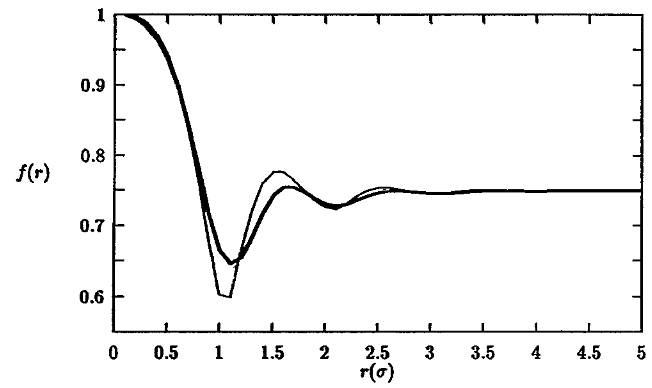

FIG. 3. Screening functions for an electron solvated in a hard sphere fluid of reduced density $\rho^*=0.8$ and reduced polarizability $\alpha^*=0.06$. (a) The solid curve is calculated from Eq. (4.35); (b) the bold curve is calculated from Eq. (4.42).

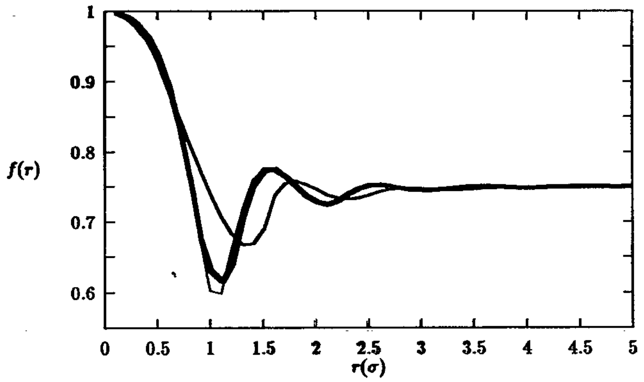

FIG. 4. Screening functions calculated from Eq. (4.35) for an electron solvated in a hard sphere fluid of reduced density $\rho^*=0.8$ and reduced polarizability $\alpha^*=0.06$. The electron–solvent pair correlation functions are taken as a step function $g_e(r)=\theta(r-d)$. (a) The solid curve corresponds to $d=0$; (b) the very bold curve corresponds to $d=0.2$; (c) the bold curve corresponds to $d=0.5$.

tion of solvent $g(R)$ can be computed by solving the OZ equation subject to hard sphere closure.[33] We assume that the fluid is unperturbed by the presence of the electron so that the electron–solvent pair correlation function g_e is taken to be 1. It is of interest to determine whether the screening function will be sensitive to the assumption $g_e=1$.

We now take g_e as a step function $g_e=\theta(r-d)$. In Fig. 4, several screening functions calculated from Eq. (4.35) are plotted for different choices of d. Obviously if d is small, the solvent is less perturbed by the electron and thus the screening function is very similar to that for $g_e=1$. In the context of the FEBO approximation, g_e is the electron bead–solvent particle pair correlation function, a quantity already determined for electron solvation in He and Xe liquids at several temperatures and densities in the pair polarization approximation.[30] The inclusion of the many-body polarization energy [Eq. (4.34)] might alter g_e and will thus affect the screening function. This suggests a self-consistent treatment in which g_e already determined is used to calculate $f(r)$ using Eq. (4.35) or Eq. (4.42) and the resulting $f(r)$ is then used in the simulations to compute g_e. This procedure is iterated to the final solution. However, it is possible that such a procedure will be unnecessary because of the following:

(a) The solvent structure is determined mainly by the short-range repulsive potential. The effect of the polarization energy on the screening functions is a second order effect.

(b) From the previous simulation results,[30] g_e at high solvent densities is very close to a step function with a small interaction diameter d, smaller than the effective switching range of $c(r)$. We can thus approximate it by $g_e=1$.

The ground state energy E_0 as a function of solvent density can be computed based on the FEBO approximation (2.11) and the mean field approximation of the polarization energy (4.34). Preliminary results indicate that Lekner's mean field theory and the matrix inversion method agree within 10% and that the screening function calculated from Eq. (4.42) results in a decrease in E_0 compared to E_0 calculated from Eq. (4.35). Details of the simulation results and relevant discussions will be presented in a future paper.

APPENDIX A

1. A simple illustrative quadratic model of particles interacting with slow quantum field

The canonical partition function for a quantum particle moving in an external potential $V(x)$ interacting with another quantum system is

$$Z=\int dx \int [\mathscr{D}x(u)]\exp\{-S[x(u)]\}, \tag{A1}$$

where u measures the Euclidean time $t=i\hbar\beta u$ and S is the Euclidean action given by

$$S=\beta\int_0^1 \left\{\frac{m}{2\beta^2\hbar^2}\dot{x}^2+V[x(u)]+V_{\text{int}}[x(u),u]\right\}du, \tag{A2}$$

in which m is the mass of the particle. Our goal is to demonstrate that Eq. (A1) can be reduced to the form (2.21) under adiabatic conditions.

We assume that V is a bounded potential much stronger than the interaction potential V_{int}, so that the energy levels are dominated by V. Taylor expansion of the potential to quadratic order yields

$$\begin{aligned} V&=V_0+V_1x+\frac{m\omega^2}{2}x^2+\cdots, \\ V_{\text{int}}&=e(u)-f(u)x-\frac{W(u)}{2}x^2+\cdots, \end{aligned} \tag{A3}$$

where V_0, V_1, and $m\omega^2$ are the zeroth, first, and second derivatives of the potential V, respectively, and $e(u)$, $-f(u)$, and $-W(u)$ are the zeroth, first, and second derivatives of V_{int}, respectively. Substitution of these expansions into the action (A2) gives

$$S=\beta\int_0^1\left[\frac{m}{2\hbar^2\beta^2}\dot{x}^2+\frac{m\omega^2}{2}x^2+E(u)-F(u)x-\frac{W(u)}{2}x^2\right]du \tag{A4}$$

where $F(u)=f(u)-V_1$, $E(u)=e(u)+V_0$.

The normal-mode transformation defined by

$$x(u)=\sum_{n=-\infty}^{\infty}\tilde{x}_n\exp(-i2\pi nu) \tag{A5}$$

allows Eq. (A4) to be expressed as

$$S=\beta\left\{\tilde{E}_0+\sum_n\frac{m\omega^2}{2}\left[\left(\frac{2\pi n}{b}\right)^2+1\right]|\tilde{x}_n|^2-\sum_n\tilde{F}_n^*\tilde{x}_n-\sum_{nm}\frac{1}{2}\tilde{x}_n^*\tilde{W}_{nm}\tilde{x}_m\right\}, \tag{A6}$$

where the tilde denotes the corresponding normal-mode variables, and where $b=\beta\hbar\omega$ is the ratio of the energy level spliting of the quadratic potential V [defined in Eq. (A3)] to the thermal energy kT.

Substitution of Eq. (A6)

$$\sigma_n=\frac{1}{m\omega^2}\left[\left(\frac{2\pi m}{b}\right)^2+1\right]^{-1}, \tag{A7}$$

and the matrix

$$C_{nm}=\delta_{nm}-\sqrt{\sigma_n}\tilde{W}_{nm}\sqrt{\sigma_m}, \tag{A8}$$

into Eq. (A2) followed by explicit evaluation of the Gaussian integrals gives

$$Z=Z_0\exp(-\beta\tilde{E}_0+I+J), \tag{A9}$$

where $Z_0=[2\tanh(b/2)]^{-1}$ is the partition function of a LHO of frequency ω, and I and J are

$$I=-\tfrac{1}{2}\ln(C) \tag{A10}$$

and

$$J=\frac{\beta\tilde{F}\sqrt{\sigma}C^{-1}\sqrt{\sigma}\tilde{F}}{2}. \tag{A11}$$

When the quantum source giving rise to the interaction potential V_{int} is slow compared to the quantum variable x, I and J can be reduced to simple expressions. The identity $\ln(\det C)=\text{Tr}\ln C$ and a Taylor expansion gives

$$I=\sum_l I_l=\sum_l\frac{1}{2l}\text{Tr}(\sqrt{\sigma}\tilde{W}\sqrt{\sigma})^l. \tag{A12}$$

Transformation of I_l back to the imaginary time space then gives

$$I_l=\sum_{i=1}^{l}\left(\int_0^1 du_i\right)\sigma(u_1-u_2)W(u_2)\sigma(u_2-u_3)\times W(u_3)\cdots\sigma(u_l-u_1)W(u_1), \tag{A13}$$

where $\sigma(u)$ is the transform of σ_n,

$$\sigma(u)=\sigma_0\frac{b/2}{\sinh(b/2)}\cosh(b/2-b|u|), \tag{A14}$$

in which $\sigma_0=1/m\omega^2$ is the Gaussian width of the zeroth mode in the classical limit.

When b is large, $\sigma(u)$ is a rapidly decaying function of u and $W(u)$ will decay slowly compared to $\sigma(u)$. Then $W(u)$ is essentially a constant, while $\sigma(u)$ varies over the range $1/b$ and Eq. (A14) can be approximated by

$$I_l=\int_0^1 W^l(u)du\left[\prod_{i=1}^{l-1}du_i\sigma(u_1)\sigma(u_2)\cdots\sigma(u_{l-1})\times\sigma(u_1+u_2+\cdots+u_{l-1})\right]. \tag{A15}$$

The integration in the square bracket can be evaluated by transforming back to the normal mode space to give $\Sigma_n\sigma_n^l$ and then summing over the normal modes giving

$$I_l=\frac{b}{2}C_l(b)\int(\sigma_0 W)^l du, \tag{A16}$$

where $C_l(b)$ is defined as

$$\sum_n\frac{1}{l}\left[\frac{1}{1+(2\pi n/b)^2}\right]^l=bC_l(b), \tag{A17}$$

and where

$$\lim_{b\to\infty}C_l(b)=\frac{(2l-3)!!}{(2l)!!}. \tag{A18}$$

Taylor expansion of J gives

$$J=\sum_l J_l=\sum_{l=0}^{\infty}\frac{\beta}{2}\tilde{F}\sqrt{\sigma}(\sqrt{\sigma}W\sqrt{\sigma})^l\sqrt{\sigma}\tilde{F}. \tag{A19}$$

Transforming each I_l back to the imaginary time space gives

$$J_l=\frac{\beta}{2}\int\prod_{i=1}^{l+2}du_i F(u_1)\sigma(u_1-u_2)W(u_2)\times\sigma(u_2-u_3)\cdots F(u_{l+2}). \tag{A20}$$

The same arguments used to derive Eq. (A16) can be used to show that J_l reduces to

$$J_l=\frac{\beta}{2}\int f(u)W^l(u)f(u)du\times\left[\int\prod_{i=1}^{l+1}du_i\sigma(u_1)\cdots\sigma(u_{l+1})\right], \tag{A21}$$

where the integrations in the brackets are simply $(\sigma_0)^{l+1}$.

Substitution of Eqs. (A16) and (A21) into Eq. (A9) yields the quantum partition function

$$Z=Z_0\exp\left(-\beta\int\left\{E(u)-\frac{1}{2}F^2(u)[1-\sigma_0 W(u)]^{-1}-\sum_l\frac{\hbar\omega}{2}C_l(b)[\sigma_0 W(u)]^l\right\}du\right), \tag{A22}$$

where $(1-\sigma_0 W)^{-1}$ is the result of the summation over l.

Equation (A22) is significant because it is purely local in time and does not depend on time-correlation functions as is usually the case. For example, if a cumulant expansion is made, one obtains terms such as $\int du \int du' V(u)V(u')$ as well as higher orders. The exponential part of Eq. (A22) is simply the linear summation of the contributions from individual time slices. This confirms the free energy adiabatic approximation we introduced in Eq. (2.21). It implies that in the discretized time expression, beads at different time slices do not interact.

The problem can be easily translated into a real time formulation and the same conclusion holds. If the quantum source of V_{int} is very slow compared to the oscillators, the oscillators can respond to the field almost instantaneously.

APPENDIX B: CUMULANT EXPANSION (*I*)

The FEBO approximation given by Eq. (2.11) is in fact the first order approximation. Higher order terms can be included by using perturbation theory. Consider the Hamiltonian (2.1), where $H_x=m_x\dot{x}^2/2$ and $H_y=m_y\dot{y}^2/2$ are the free particle Hamiltonians of the fast and slow variables, respectively. The slow and fast variables differ only in masses, so we expect that higher order corrections involve powers of $\eta=m_x/m_y$.

First we put the slow variable aside and integrate the fast variable. Expressing the variable as $x(u)=x_0+\delta x(u)$, the action reads

$$S_x=\beta\int\left[\frac{\dot{\delta x}^2 m}{2\hbar^2\beta^2}+V(x_0+\delta x,u)\right]du, \tag{B1}$$

where the potential depends on u in general. For the sake of simplicity, we omit the subscript x without causing any confusion and we will recover the subscript later on when the other variable y is present in the expression explicitly.

We choose to use the centroid density $\rho^*(x_0)$ (Ref. 22)

$$\rho^*(x_0)=\rho^*_{\text{free}}\left\langle \exp\left[-\beta\int V[x_0+\delta x(u),u]du\right]\right\rangle$$
$$=\rho^*_{\text{free}}e^{-\beta V_{\text{eff}}} \tag{B2}$$

to confine the free particle reference system, where $\rho^*_{\text{free}}=\sqrt{m/(2\pi\hbar^2\beta)}$ and the average is defined in the free particle reference system.

The average of the exponential can be written as a cumulant expansion which leads to an expansion of the effective potential. The definitions of cumulants C_l and moments I_l, and their relations are given by Eqs. (2.15)–(2.19) in our previous paper.[22] After performing a normal mode expansion of the path and a Fourier expansion of the potential, the first moment becomes

$$I_1=\int\frac{\int V(x_0+\delta x,u)\exp(-\delta x^2/2\sigma^2)d\delta x}{\int\exp(-\delta x^2/2\sigma^2)d\delta x}du, \tag{B3}$$

where the Gaussian with σ is

$$\sigma^2=\frac{\beta\hbar^2}{12m}, \tag{B4}$$

and the second moment becomes

$$I_2=\iint\frac{\int\int V(x_0+\delta x_1,u_1)V(x_0+\delta x_2,u_2)P(\delta x_1,\delta x_2,u_1,u_2)d\delta x_1\,d\delta x_2}{\int\int V(x_0+\delta x_1,u_1)V(x_0+\delta x_2,u_2)d\delta x_1\,d\delta x_2}du_1\,du_2 \tag{B5}$$

in which the two-variable distribution function is found to be

$$P(\delta x_1,\delta x_2,u_1,u_2)=\exp\left[-\frac{\sigma^2\delta x_1^2+\sigma^2\delta x_2^2-2\sigma_c^2\delta x_1\delta x_2}{2(\sigma^4-\sigma_c^4)}\right], \tag{B6}$$

where the Gaussian width of the cross term σ_c is a function of the imaginary time

$$\sigma_c^2(u_1,u_2)=\sigma^2[1-6v(1-v)], \tag{B7}$$

where $v=|u_1-u_2|$.

Under the adiabatic approximation, the Euclidean time dependence of the quantum potential $V(u)$ is ignored so that the integration with respect to u in Eqs. (B3) and (B5) can be easily completed. In other words, we are solving a problem of a quantum particle moving in a classical potential which varies with the slow variable y adiabatically [cf. Eq. (2.12)]. Expanding the moments in a power series in β and substituting this into cumulant relations, we determine the expansion of the effective potential up to order of β^3,

$$V-\text{eff}=\hat{L}V$$
$$=V+\frac{\sigma^2}{2}V^{(2)}+\frac{\sigma^4}{8}V^{(4)}+\frac{\sigma^6}{48}V^{(6)}-\beta\frac{\sigma^4}{20}(V^{(2)})^2$$
$$+O(\beta^4) \tag{B8}$$

and the centroid density can be approximated to the same order. The effective potential V_{eff} results from the operation $\hat{L}$ on V.

Consider the full Hamiltonian of the system, the cumulant expansion shall be carried out twice, first with respect to the slow variable and second with respect to the fast variable. Under the adiabatic approximation, the two expansions are independent so that the effective potential can be obtained by operating with $\hat{L}$ on V twice

$$V_{\text{eff}}(x_0,y_0)=\hat{L}\left(\sigma_y,\frac{\partial}{\partial y}\right)\hat{L}\left(\sigma_x,\frac{\partial}{\partial x}\right)V$$
$$=V+\frac{1}{2}\,(\sigma_x^2V^{(2,0)}+\sigma_y^2V^{(0,2)})+\frac{1}{8}\,(\sigma_x^4V^{(4,0)}+2\sigma_x^2\sigma_y^2V^{(2,2)}+\sigma_y^4V^{(0,4)})+\frac{1}{48}\,(\sigma_x^6V^{(6,0)}+3\sigma_x^4\sigma_y^2V^{(4,2)}$$
$$+3\sigma_x^2\sigma_y^4V^{(2,4)}+\sigma_y^6V^{(0,6)})-\frac{\beta}{20}\,[\sigma_x^4(V^{(2,0)})^2+\sigma_y^4(V^{(0,2)})^2]+O(\beta^4), \tag{B9}$$

where $V^{(n,m)}=\partial_x^n\partial_y^m V(x_0,y_0)$.

Now we make the full quantum calculation (2.20) without the adiabatic approximation (2.12). The leading term in the second cumulant C_2 is

$$C_2=\int du_1\int du_2\sigma_c^2(v)V^{(1)}(u_1)V^{(1)}(u_2) \tag{B10}$$

which vanishes under adiabatic approximation. However, V does depend on u implicitly through $y(u)$. Thus this term in C_2 shall be evaluated after further averaging over the y paths. Applying Eq. (B8) to obtain a cumulant expansion with respect to the slow variable y, we have the leading term of the nonadiabatic correction

$$\delta V_{\text{eff}}=-\frac{1}{2}\beta(V^{(1,1)})^2\int du_1\int du_2\sigma_{c,x}\sigma_{c,y}$$
$$=-\frac{1}{20}\beta(V^{(1,1)})^2\sigma_x^2\sigma_y^2. \tag{B11}$$

To estimate the error introduced by the adiabatic approximation, we compare δV_{eff} with the terms of the same order in Eq. (B9), thus defining the error as

$$\epsilon(x_0,y_0)=\frac{2\sigma_x^2\sigma_y^2(\partial_x\partial_yV)^2}{\sigma_x^4(\partial_xV)^4+\sigma_y^4(\partial_yV)^4}. \tag{B12}$$

If the interaction potential only depends on the relative coordinate, the partial derivative terms of the potential in Eq. (B12) are the same, so that the error becomes

$$\epsilon=\frac{2\sigma_x^2\sigma_y^2}{\sigma_x^4+\sigma_y^4}=\frac{2\eta}{\eta^2+1}, \tag{B13}$$

where $\eta=m_x/m_y$. The error reaches a maximum when $\eta=1$, and decreases as $\epsilon\to 2\eta$ when $\eta\ll 1$. If the masses are very different, the error introduced by the adiabatic approximation is small and proportional to the mass ratio η.

The nonadiabatic correction comes from the interference of the two quantum particles, whereas the adiabatic approximation treats the two quantum particles independently. In the limit of small mass ratio $\eta\to 0$, the error has the asymptotic form $\epsilon=O(\eta)$. Generally speaking, the adiabatic approximation is best when the time scales of two subsystems are very different because then the subsystems are weakly coupled and the quantum interference is small.

APPENDIX C: CUMULANT EXPANSION (II)

If the reference system is two uncoupled linear harmonic oscillators, the separation of time scales is given by the ratio of the frequencies $\eta=\omega_y/\omega_x$. We used to study a Drude oscillator system; the reference system based on the LHO is relevant. The full Hamiltonian is then given by Eq. (2.1) in which $H_x=m_x\dot{x}^2/2\hbar^2\beta+m_x\omega_x^2x^2/2$, $H_y=m_y\dot{y}^2/2(\hbar\beta)^2+m_y\omega_y^2y^2/2$. Since the harmonic oscillator has a well defined partition function, we determine an effective potential for the partition function and will thus not treat the centroid density as in the last section.

Following the same procedure described in last section, we first integrate the fast variable x, the action of which is

$$S_x=\beta\int\left\{\frac{m\dot{x}^2}{2\hbar^2\beta^2}+\frac{m\omega^2\dot{x}^2}{2}+V[x(u),u]\right\}du. \tag{C1}$$

Again, for the sake of simplicity, we omit the subscript x without causing any confusion. And the partition function for the fast variable reads

$$Z=Z_{\text{LHO}}\left\langle\exp\left\{-\beta\int V[x(u),u]du\right\}\right\rangle=Z_{\text{LHO}}e^{\beta V_{\text{eff}}}, \tag{C2}$$

where the average is defined in the LHO reference system and where $Z_{\text{LHO}}=\coth(b/2)/2$ is the quantum partition function for the LHO ($b=\hbar\omega\beta$).

The same cumulant expansion applies here. The general results in last section I_1 of Eq. (B3) and I_2 of Eq. (B6) hold exactly for the LHO reference system except that the two Guassian widths are now

$$\sigma^2=\frac{\hbar^2\beta}{2mb}\,\frac{1}{\tanh(b/2)} \tag{C3}$$

and

$$\sigma_c^2(u_1,u_2)=\sigma^2\,\frac{\cosh(1/2-v)b}{\cosh(b/2)}. \tag{C4}$$

Now the adiabatic approximation allows us to ignore the u dependence of the potential V so that the integration of σ_c can be readily carried out

$$\bar{\sigma}_c^2=\int\int\sigma_c^2\,du_1\,du_2=\frac{\tanh(b/2)}{b}\,\sigma^2 \tag{C5}$$

and

$$\bar{\sigma}_c^4=\iint \sigma_c^4\, du_1\, du_2=\frac{1+\sinh(b)/b}{2[\cosh(b/2)]^2}\,\sigma^4. \tag{C6}$$

Thus the effective potential up to β^3 is

$$\hat{L}V=V+\frac{\sigma^2}{2}\,V^{(2)}+\frac{\sigma^4}{8}\,V^{(4)}+\frac{\sigma^6}{48}\,V^{(6)}-\beta\frac{\bar{\sigma}_c^2}{2}\,(V^{(1)})^2 -\beta\frac{\bar{\sigma}_c^4}{4}\,(V^{(2)})^2-\beta\frac{\bar{\sigma}_c^2\sigma^2}{8}\,(V^{(3)}V^{(1)})+O(\beta^4), \tag{C7}$$

in which values of the potential and its derivatives are taken at $x=0$.

Next consider the full action; under the adiabatic approximation (2.11) the full effective potential can be obtained by applying the the operator $\hat{L}$ twice to get

$$V_{\text{eff}}=\hat{L}_y\hat{L}_xV=\cdots-\frac{\beta}{2}\,(\sigma_x^2\bar{\sigma}_{y,c}^2+\sigma_y^2\bar{\sigma}_{x,c}^2)\,(\partial_x\partial_yV)^2+\cdots, \tag{C8}$$

where only relevant terms which will be useful later are explicitly given. The leading nonadiabatic term takes the same form as Eq. (B11), and the integration can be performed to give

$$\iint \sigma_{x,c}^2\sigma_{y,c}^2 du_1\, du_2 =\sigma_x^2\sigma_y^2\,\frac{2[b_x\tanh(b_x/2)-b_y\tanh(b_y/2)]}{b_x^2-b_y^2}, \tag{C9}$$

so that the correction to the effective potential is

$$\delta V_{\text{eff}}=-\beta\sigma_x^2\sigma_y^2\,\frac{2[b_x\tanh(b_x/2)-b_y\tanh(b_y/2)]}{b_x^2-b_y^2}. \tag{C10}$$

Comparing δV_{eff} with the similar terms in V_{eff} expansion, we have the error

$$\epsilon=\frac{2[b_x\tanh(b_x/2)-b_y\tanh(b_y/2)]/(b_x^2-b_y^2)}{\tanh(b_x/2)/b_x+\tanh(b_y/2)/b_y}\,(\partial_x\partial_yV)^2. \tag{C11}$$

In the low temperature limits $b_x \gg 1$ and $b_y \gg 1$, we take $\tanh(b_x/2)$ and $\tanh(b_y/2)$ to be 1. Then the error becomes

$$\epsilon=\frac{2b_xb_y}{(b_x+b_y)^2}=\frac{2\eta}{(\eta+1)^2}, \tag{C12}$$

which reaches its maximum 1/2 at $\eta=1$ and decreases as $\epsilon \to 2\eta$ at small η limit.

From the results of these two appendices, we can draw the conclusion that the error of the FEBO approximation is asymptotically proportional to the ratio of the time scales, and this ratio of time scales is characterized by a parameter η, the ratio of masses for the molecules, or the ratio of frequencies for the Drude oscillator systems.

APPENDIX D: THE VIRIAL ESTIMATOR FOR NMPIMC

Here we derive the virial estimator for Eq. (3.10). As is known, energy can be deduced from the derivative of the partition function with respect to β, i.e.,

$$E=-\frac{\partial}{\partial\beta}\ln Z, \tag{D1}$$

which yields

$$E=\left\langle \sum_{j=1}^{P}\left[\frac{R}{2\beta\tanh(R)}-\frac{PR^2\cosh(R)}{2\lambda'^2\beta[\sinh(R)]^2}\,(x_j-x_{j-1})^2 +\frac{PR^2[\cosh(R)-1]}{2\lambda'^2\beta[\sinh(R)]^2}\,(x_j^2+x_{j-1}^2)+\frac{1}{P}\,V'(x_j)\right]\right\rangle, \tag{D2}$$

where $\langle f\rangle$ denotes the average over the P dimensional space with the weighting function e^{-S}. The simple identity $\langle\Sigma_{j=1}^P x_j[(\partial S)/(\partial x_j)]\rangle=P$ leads to

$$P=\sum_{j=1}^{P}\left\langle\frac{PR}{\lambda'^2\sinh(R)}\,\{(x_j-x_{j-1})^2+(x_j^2+x_{j-1}^2) \times[\cosh(R)-1]\}+\frac{\beta}{P}x_j\,\frac{\partial V'}{\partial x_j}\right]\right\rangle. \tag{D3}$$

Combining Eqs. (D2) and (D3) and rearranging the terms, we arrive at the virial estimator

$$E(\beta,P)=\sum_{j=1}^{P}\frac{1}{P}\left\langle m\omega^2x_j^2+V(x_j)+\frac{R}{2\tanh R}\,x_j\,\frac{\partial V'}{\partial x_j}\right\rangle \tag{D4}$$

in which the first term is obviously due to the LHO potential and the second term is due to the residue potential.

APPENDIX E: QUANTUM CALCULATION OF THE PROTOTYPE POTENTIAL

Let us introduce α' as

$$\alpha'=\frac{eq}{m\omega^2} \tag{E1}$$

so that Eq. (4.17) can be written as $V=m\omega^2U$, where U is given by

$$U=\frac{\mathbf{r}^2}{2}+\alpha'\left(\frac{1}{|\mathbf{R}-\mathbf{r}|}-\frac{1}{R}\right). \tag{E2}$$

First we locate the minimum of the potential V by taking the first order derivative of U with respect to the vector $\mathbf{r}$,

$$\frac{\partial U}{\partial r_i}=r_i+\alpha'\,\frac{R_i-r_i}{|\mathbf{R}-\mathbf{r}|}, \tag{E3}$$

which vanishes at the equilibrium position r_i' given by

$$x'=-\frac{\alpha'}{(R-x')^2},\quad y'=0,\quad z'=0. \tag{E4}$$

Therefore the leading order of the energy shift is the minimum potential

$$\Delta E_{\min}=V(r_i'). \tag{E5}$$

At large separation, we can approximately solve Eq. (E4) by expanding $\alpha'/(R-x')^2$ to the second order in x', and substitution of r_i' into Eq. (E2) yields

$$U_{\min}=-\frac{\alpha'^2}{2R^4}\frac{1}{(1+2\alpha'/R^3)}, \tag{E6}$$

which implies that the expansion is valid only if $R^3\gg\alpha'$. Obviously the first factor of the right-hand side of Eq. (E6) is the interaction energy ΔE_d under the dipolar approximation and the second factor is the correction function $c(R)$ defined in Eq. (4.21) However, comparison with the accurate results from simulations indicates that $c(R)=1/(1+2\alpha'/R^3)$ does not give the right asymptotic behavior because the simulated $c(r)$ approaches 1 from above.

To obtain the leading order correction, we shall carry out the quantum expansion to the next order

$$\frac{\partial^2 U}{\partial r_i'\partial r_j'}=\delta_{ij}\left[1+(3\delta_{i1}\delta_{j1}-1)\frac{\alpha'}{(R-x')^3}\right], \tag{E7}$$

which defines the eigenfrequencies of the motion around the potential minimum. As an isolated Drude oscillator has the ground energy of $3\hbar\omega/2$, the frequency shift gives the second order corrections as

$$\Delta E_\omega=\frac{\hbar\omega}{2}\left(\mathrm{Tr}\sqrt{\frac{\partial^2 U}{\partial r_i'\partial r_j'}}-3\right). \tag{E8}$$

Now at large R limit, the leading order correction in the energy is

$$\Delta E_{R^3\gg\alpha'}=m\omega U_{\min}-\frac{3}{8}\hbar\omega\alpha'^2\frac{1}{R^6}, \tag{E9}$$

and thus the asyptotic behavior of the correction function $c(r)$ at large distance is

$$\lim_{R\to\infty} c(r)=1+O(1/R^6). \tag{E10}$$

Also applying Eqs. (E5)–(E8), we are able to predict that the energy shift at short distance $R^3\ll\alpha'$ is $U_{R\to 0}=-\alpha'/R$, which indicates the correction function approachs the origin as

$$\lim_{R\to 0} c(r)=O(R^2). \tag{E11}$$

To further improve the accuracy, we notice the potential well at the minimum r_i' is not exact harmonic especially at small R where there is a large anharmonicity. To take account of this effect, we shall expand the potential (4.17) to the third order and evaluate its contribution by quantum perturbation theory. The unperturbed Hamiltonian is that of the harmonic oscillator whose frequencies are given by Eq. (D7), and the perturbation Hamiltonian is written as

$$H'=\frac{1}{3!}\sum_{ijk}\partial_i\partial_j\partial_k V(\mathbf{r}')\delta r_i\delta r_j\partial_k, \tag{E12}$$

where the third order derivative is

$$\partial_i\partial_j\partial_k V(\mathbf{r}')=eq\left[\frac{15R_i'R_j'R_k'}{R'^7}-\frac{3}{R'^5}(\delta_{ij}R_k'+\delta_{jk}R_i'+\delta_{ki}R_j')\right], \tag{E13}$$

in which $\mathbf{R}'=\mathbf{R}-\mathbf{r}'$. It is easy to observe that all the terms in Eq. (E13) vanish except terms with indices $i=j=k=1$ and $i=1$, $j=k=2$ or $i=1$, $j=k=3$ and corresponding permutation terms. Since H' is odd order in δr, the first nonvanishing perturbation term is

$$\Delta E_3=-\sum_n\frac{\langle n|H'|0\rangle^2}{E_0-E_n}, \tag{E14}$$

where n stands for the index of the eigenstates of the unperturbed Hamiltonian and E_0 is the corresponding energy eigenvalue. Obviously, ΔE_3 further lower the energy and its leading contribution is of the order of $O(1/R^{10})$ at large separation R.

Finally, the ground state energy shift is given by

$$\Delta E=\Delta E_{\min}+\Delta E_\omega+\Delta E_3. \tag{E15}$$

The correction function (4.21) thus calculated is plotted in Fig. 2.

[1] B. J. Berne and D. Thirumalai, Annu. Rev. Phys. Chem. **37**, 401 (1986). For references on Path Integral Monte Carlo, see the papers cited here.

[2] J. Hoye and G. Stell, J. Chem. Phys. **73**, 461 (1980).

[3] G. S. Rushbrooke, G. Stell, and J. S.Hoye, Mol. Phys. **26**, 1200 (1973).

[4] E. L. Pollack and B. J. Alder, Phys. Rev. Lett. **39**, 299 (1977).

[5] L. R. Pratt, Mol. Phys. **40**, 347 (1980).

[6] D. Chandler, K. S. Schweizer, and P. G. Wolynes, Phys. Rev. Lett. **49**, 1100 (1982).

[7] Z. Chen and R. M. Stratt, J. Chem. Phys. **95**, 2669 (1991).

[8] D. E. Logan, Mol. Phys. **51**, 1365 (1984).

[9] Z. Chen and R. Stratt, J. Chem. Phys. **95**, 2669 (1991).

[10] B. Cichocki, B. U. Felderhof, and K. Kinsen, Phys. Rev. A **39**, 5350 (1989).

[11] B. Space, D. F. Coker, Z. H. Liu, B. J. Berne, and G. Martyna, J. Chem. Phys. **97**, 2002 (1992).

[12] A. L. Nichols III and D. Chandler, J. Chem. Phys. **84**, 398 (1986).

[13] J. Lekner, Phys. Rev. **158**, 130 (1967).

[14] A. S. Davydov, *Quantum Mechanics* (Pergamon, New York, 1965).

[15] R. P. Feynman and A. R. Hibbs, *Quantum Mechanics and Path Integral* (McGraw–Hill, New York, 1965).

[16] M. Suzuki, Commun. Math. Phys. **51**, 183 (1976).

[17] H. De Raedt and B. De Raedt, Phys. Rev. A **28**, 3575 (1983).

[18] M. Takashi and M. Imada, J. Phys. Soc. Jpn. **53**, 3765 (1984).

[19] M. J. Thompson, K. S. Schweizer, and D. Chandler, J. Chem. Phys. **76**, 1128 (1982).

[20] D. Chandler, Y. Singh, and D. M. Richardson, J. Chem. Phys. **81**, 1975 (1984).

[21] G. A. Voth, D. Chandler, and W. H. Miller, J. Chem. Phys. **91**, xxxx (1989).

[22] J. Cao and B. J. Berne, J. Chem. Phys. **92**, 7531 (1990).

[23] R. D. Coalson, D. L. Freeman, and J. D. Doll, J. Chem. Phys. **85**, 4567 (1986).

[24] J. D. Doll, D. L. Freeman, and T. L. Beck, Adv. Chem. Phys. **78**, 61 (1990).

[25] M. F. Herman, E. J. Bruskin, and B. J. Berne, J. Chem. Phys. **76**, 5150 (1982).

[26] M. L. Klein, M. Sprik, and D. Chandler, Phys. Rev. **31**, 4243 (1985).

[27] J. A. Barker, in *Rare Gas Solids*, edited by M. L. Klein and J. A. Venables (Academic, New York, 1984).

[28] J. Miyazaki, J. A. Barker, and G. M. Pound, J. Chem. Phys. **64**, 3364 (1976).

[29] J. Cao and B. J. Berne, J. Chem. Phys. **97**, 8628 (1992).

[30] D. F. Coker, B. J. Berne, and D. Thirumalai, J. Chem. Phys. **86**, 5689 (1987).

[31] M. New and B. J. Berne (unpublished results).

[32] Z. Liu and B. J. Berne (unpublished results).

[33] J. P. Hansen and I. R. McDonald, *Theory of Simple Fluids* (Academic, New York, 1986).